NEUROSCIENCE
RESEARCH ARTICLE
X. Ma et al. / Neuroscience 425 (2020) 1–11

Altered Temporal Organization of Brief Spontaneous Brain Activities in Patients with Alzheimer's Disease

Xiangyu Ma,[a,b] Zhizheng Zhuo,[a,b] Lijiang Wei,[a,b] Zhe Ma,[a,b] Zhaoxia Li[c] and Haiyun Li[a,b]*, Alzheimer's Disease Neuroimaging Initiative[†]

[a] *School of Biomedical Engineering, Capital Medical University, Beijing, China*

[b] *Beijing Key Laboratory of Fundamental Research on Biomechanics in Clinical Application, Capital Medical University, Beijing 10069, China*

[c] *School of Chinese Medicine, Capital Medical University, Beijing, China*

Abstract—The alterations of dynamic brain functions in Alzheimer's disease (AD) remain far from well understood. In this study, using functional magnetic resonance imaging (fMRI) data, we adopted a co-activation pattern (CAP) approach, which relies on very few assumptions, to explore the differences of brain dynamics among healthy elderly, patients with early amnestic mild cognitive impairment (MCI) and patients with AD. Briefly, k-means clustering was applied to all fMRI frames from the three groups and generated a set of reproducible CAPs. We found the obtained CAPs showed high correspondence to the well acknowledged functional networks including default mode network (DMN), executive control network and visual networks, etc. Different from previous CAP-based studies, we further quantitatively analyzed the temporal dependence of the CAPs using multiple parameters. Primary findings include, for AD and MCI compared with NC, the decreased mean fraction of occurrence and persistence of DMN related CAPs, which indicates the typical DMN damage; the increased/decreased mean persistence of ventral/dorsal visual network related CAPs, which may associate with the visuospatial disorder of patients with AD pathology; the elevated transition and CAP entropies and multiple alterations of CAP transition probabilities, which imply the altered mode of information flow and lifted system uncertainty in AD brains. We also found correlations of proposed measurements to cerebrospinal fluid biomarkers and neuropsychological scores. This study verified the AD-related alteration found by traditional FC analysis, and proposed several new biomarkers which have the potential for assisting AD treatment and early diagnosis. **© 2019 IBRO. Published by Elsevier Ltd. All rights reserved.**

Key words: Alzheimer's disease, functional magnetic resonance imaging, default mode network, visual network, co-activation pattern, temporal dependence.

INTRODUCTION

Alzheimer's disease (AD) is a neurodegenerative disease with great threat to the elderly. Although the progression of AD is thought to be not reversible, the early diagnosis of AD is important to maximize the benefit of treatment and lifestyle prevention strategies for AD. Unfortunately, according to the current clinical criteria, AD diagnosis is only made when a patient has suffered from dementia which corresponds to the late stage of AD (Belleville et al., 2017; Boland, 2015; McKhann et al., 2011). To this end, it is crucial to better understand AD mechanism and identify AD specific brain abnormality especially at its earlier stage, also known as mild cognitive impairment (MCI).

Functional magnetic resonance imaging (fMRI) could provide time-resolved information about brain spontaneous activity with high spatial resolution which enables us to explore the interactions among brain regions. With fMRI time series, relationship between neural activities of different regions can be estimated by calculating their functional connectivities (FCs). Typically, brain networks constructed by FCs computed from long or full length of fMRI series are known as long-term or static networks. Among them, default mode network (DMN) has been mostly reported to be relevant to AD and disruptions in the DMN may lead to typical AD symptoms since the close relationship between

*Corresponding author.
E-mail address: haiyunli@ccmu.edu.cn (H. Li).

[†] Data used in preparation of this article were obtained from the Alzheimer's Disease Neuroimaging Initiative (ADNI) database (adni.loni.usc.edu). As such, the investigators within the ADNI contributed to the design and implementation of ADNI and/or provided data but did not participate in analysis or writing of this report. A complete listing of ADNI investigators can be found at: http://adni.loni.usc.edu/wp-content/uploads/how_to_apply/ADNI_Acknowledgement_List.pdf.

Abbreviations: AD, Alzheimer's disease; CAP, co-activation pattern; DMN, default mode network; FCs, functional connectivities; fMRI, functional magnetic resonance imaging; HMM, hidden Markov model; MCI, mild cognitive impairment.

https://doi.org/10.1016/j.neuroscience.2019.11.025
0306-4522/© 2019 IBRO. Published by Elsevier Ltd. All rights reserved.

DMN and memory formation and retrieval (Banks et al., 2018; Buckner et al., 2008; Qi et al., 2018).

Long-term functional networks can reflect static brain functional patterns; however, these interpretations are too coarse which omit dynamic information underlying the fMRI time courses. Therefore, short-term or instantaneous brain activities and their related functional patterns have attracted more attention in recent years. Sliding window based strategies (Chang and Glover, 2010; Hutchison et al., 2013) are direct ways to extract such dynamic information whereas they always face an intrinsic problem of selecting appropriate window width and shape. In contrast, time-frame based strategies (Liu and Duyn, 2013; Smith et al., 2012; Taghia et al., 2017; Tagliazucchi et al., 2012; Vidaurre et al., 2017) avoid this problem by adopting time frame as the basic analysis unit, and therefore have the ability to capture instantaneous and dynamic information. Typically, several state-space models have been proposed recently trying to describe recurred instantaneous activities by a set of states. For example, Vidaurre et al. (2017) proposed a hidden Markov model (HMM) based method to infer such states, and discovered a hierarchical temporal structure of brain network dynamics. Smith et al. (2012) proposed a temporal ICA based method to extract temporal function modes (TFM) trying to identify functional networks based on their temporal independence. Physiological interpretation can be made according to the characteristics of the states and abundant dynamic information can be then acquired by analyzing the state time courses. However, we need to notice that the extracted states and their behaviors largely depend on the model assumptions and the robustness of the inference is affected by the model complexity and sample size.

In this study, we adopted the co-activation pattern (CAP) approach (Liu and Duyn, 2013), which relies on very few assumptions, to construct a state-space model and investigated the brain dynamics in AD, EMCI, and NC. Briefly, CAPs are a set of averaged brain activation maps calculated by clustering fMRI frames. Different from the previous studies, we focus on the temporal dependence of the CAP-constructed brain state-space.

Specifically, apart from classical measurements such as dwell time and transition probabilities of the CAPs, we proposed two novel indicators to measure the disorder degree of the brain state-space and we hypothesize that the elevated disorder degree of brain system may associate with the cognitive dysfunctions and also with the altered cerebrospinal fluid (CSF) biomarkers in patients with AD or MCI. Further, based on functional interpretations of the CAPs according to their spatial similarity to known functional networks, we discussed the possible relationships between the altered brain dynamics and the disease pathology. This research provides interesting clues for understanding the mechanism of AD, and is supposed useful for AD treatment and early diagnosis.

EXPERIMENTAL PROCEDURES

Data acquisition

Functional and structural MRI data were downloaded from the Alzheimer's disease Neuroimaging Initiative (ADNI) database (adni.loni.usc.edu). The ADNI was launched in 2003 as a public–private partnership, led by Principal Investigator Michael W. Weiner, MD. The primary goal of ADNI has been to test whether serial magnetic resonance imaging (MRI), positron emission tomography (PET), other biological markers, and clinical and neuropsychological assessment can be combined to measure the progression of MCI and early AD. The inclusion/exclusion criteria are as follows (for up-to-date information, see www.adni-info.org):

1. Normal subjects: MMSE (Mini-Mental State Examination) scores between 24 and 30 (inclusive), a CDR of 0, non-depressed, non MCI, and nondemented. The age range of normal subjects will be roughly matched to that of MCI and AD subjects.
2. Early amnestic MCI (EMCI) subjects: MMSE scores between 24 and 30 (inclusive), a memory complaint, have objective memory loss measured by education adjusted scores on Wechsler Memory Scale Logical Memory II, a CDR of 0.5, absence of significant levels of impairment in other cognitive domains, essentially preserved activities of daily living, and an absence of dementia
3. AD subjects: MMSE scores less than 24 (inclusive), a CDR greater than 0.5 (inclusive), and meets NINCDS/ADRDA criteria for probable AD (this criteria is different from the one in ADNI site for this study).

We collected the samples from the first 3 stages of ADNI—ADNI 1, ADNI-GO and ADNI 2. Totally 118 subjects who have both baseline structural and functional MRI data were included in this study of which the demographics are listed in Table 1.

All the subjects (eyes open) were scanned by 3.0-Tesla Philips MRI scanner. Resting-state functional images were obtained by echo-planar imaging sequence with following parameters: repetition time (TR) = 3000 ms; echo time (TE) = 30 ms; flip angle = 80°, number of slices = 48; slice thickness = 3.3 mm; spatial resolution = $3 \times 3 \times 3\,mm^3$ and matrix = 64×64. The length of each time series is 140 time points. T1-weighted images were acquired using a sagittal magnetization prepared rapid gradient echo (MP-RAGE) three-dimensional sequence with following parameters: slice thickness = 1.2 mm, TR = 6700 ms, TE = 3.1 ms, flip angle = 9°, matrix = $256 \times 256 \times 170$. All original image files are available to the general scientific community.

In addition, we collected the CSF biomarkers such as the accumulation of amyloid β (Aβ), tau protein (tau) and phosphorylated tau protein (p-tau), and the neuropsychological scores such as MMSE, GDS (Geriatric Depression Scale), CDR (Clinical Dementia

Table 1. Demographics of the subjects

Group	AD	EMCI	NC
Sample size	29	49	40
Age (year)[a]	74.2 ± 7.5	72.2 ± 6.7	75.0 ± 6.3
Female percentage[b]	53%	52%	55%
MMSE[c]	21.2 ± 3.4	27.9 ± 1.8	29.0 ± 1.6
GDS[d]	1.7 ± 1.6	2.1 ± 2.4	0.9 ± 1.1
CDR[e]	0.9 ± 0.3	0.5 ± 0.2	0.1 ± 0.2
FAQ[f]	16.7 ± 6.45	3.6 ± 4.9	0.7 ± 2.8
ADNI-MEM[g]	−1.0 ± 0.6	0.5 ± 0.6	1.0 ± 0.6
ADNI-EF[h]	−1.0 ± 0.7	0.5 ± 0.8	0.8 ± 0.7
Aβ (CSF, pg/ml)[i]	138.7 ± 39.3	186.6 ± 59.0	185.0 ± 50.7
Tau (CSF, pg/ml)[j]	141.7 ± 77.9	87.6 ± 68.9	72.0 ± 34.6

Key: MMSE = mini-mental state examination; Aβ (CSF), the accumulation of amyloid β in cerebrospinal fluid; ADNI-MEM, ADNI-EF: composite scores for memory and executive functioning of the ADNI cohort.

[a] One-way ANOVA among groups: $F = 1.456$, $p = 0.237$.

[b] χ^2 test for gender composition among groups: $\chi^2 = 0.320$, $p = 0.852$.

[c] One-way ANOVA among groups: $F = 108.3$, $p < 0.001$; Tamhane post hoc pairwise comparison: AD vs. EMCI, AD vs. NC, $p < 0.001$; EMCI vs. NC, $p = 0.008$.

[d] One-way ANOVA among groups: $F = 3.6$, $p = 0.031$; Tamhane post hoc pairwise comparison: AD vs. EMCI, AD vs. NC, $p > 0.05$; EMCI vs. NC, $p = 0.023$.

[e] One-way ANOVA among groups: $F = 91.6$, $p < 0.001$; Tamhane post hoc pairwise comparison: AD vs. EMCI, AD vs. NC, EMCI vs. NC, $p < 0.001$.

[f] One-way ANOVA among groups: $F = 85.7$, $p < 0.001$; Tamhane post hoc pairwise comparison: AD vs. EMCI, AD vs. NC, EMCI vs. NC, $p < 0.01$.

[g] One-way ANOVA among groups: $F = 97.0$, $p < 0.001$; Tamhane post hoc pairwise comparison: AD vs. EMCI, AD vs. NC, EMCI vs. NC, $p < 0.01$.

[h] One-way ANOVA among groups: $F = 47.3$, $p < 0.001$; Tamhane post hoc pairwise comparison: AD vs. EMCI, AD vs. NC, $p < 0.01$; EMCI vs. NC, $p > 0.05$.

[i] Kruskal–Wallis test among groups: H = 14.1, $p < 0.001$; Mann-Whitney U test for post hoc pairwise comparison: AD vs. EMCI, $p < 0.001$; AD vs. NC, $p = 0.003$; EMCI vs. NC, $p = 0.877$.

[j] Kruskal–Wallis test among groups: H = 19.3, $p < 0.001$; Mann-Whitney U test for post hoc pairwise comparison: AD vs. EMCI, $p < 0.001$; AD vs. NC, $p < 0.001$; EMCI vs. NC, $p = 0.427$.

Rating Scale), FAQ (Functional Activities Questionnaire) and two composite scores for memory (ADNI-MEM) and executive functioning (ADNI-EF) of the cohort (Gibbons et al., 2012). The mean and standard deviation of the accumulation of Aβ, tau and the neuropsychological scores of the three groups are also listed in Table 1.

Data preprocessing

Structural and functional MRI data was downloaded from public database ADNI and preprocessed complying standard fMRI preprocessing pipeline using Data Processing Assistant for Resting State fMRI (DPARSF, v3.2 advanced edition) software package(Yan and Zang, 2010). Specific preprocessing steps include slice timing, realignment (head motion correction with rigid transform), co-registering T1 images to functional images, co-variables (head motion parameters, white matter, CSF and global signals) regression, spatial normalization to MNI space and smoothing with a 4 mm FWHM Gaussian kernel (and filtering with a 0.01–0.1 Hz band pass filter). In addition, each of original functional images was binarized with a threshold to generate a mask which was also normalized into MNI space. The intersection of all the normalized masks was used to remove background voxels as well as some voxels at inferior temporal lobe and inferior frontal lobe with missing signals perhaps caused by magnetic field inhomogeneity.

Note that we did global signals regression (GSR) in this study. Some previous fMRI studies (Murphy et al., 2009a; Saad et al., 2012) suggested the global signal possibly represented some specific brain-wide activities and argued that GSR may lead to artificial results such as the anti-correlations between the task-positive networks and DMN. However, if not doing GSR, we found that the clustering process would to some extent be dominated by the global signal, hence several CAPs would exhibit strong global co-(de)activation and specific spatial organizations could not be distinguished from these CAPs.

CAP calculation

CAPs are obtained by k-means clustering on all the fMRI frames of all the subjects therefore all three groups finally share a common set of CAPs. This is for the convenience of subsequent quantitative group comparison. Before clustering, z transformation was applied therefore each voxel had a time course with mean of 0 and standard deviation of 1. Referring to the previous studies (Iraji et al., 2018; Vidaurre et al., 2017) and considering the data length of this study, we searched the initial k from 6 to 15, and the elbow criterion was used to determine the final k value to be 10 (Damaraju et al., 2014). Initial cluster centers were randomly selected from all the fMRI frames. The distances of frames to cluster centers were measured by their spatial similarities. During the clustering process, the cluster with extremely few members (< 1% of total frames) was treated as noisy cluster and discarded. The algorithm ended when the relative change of cluster centers below 0.01% or reach the maximum iteration number (80 in this study). The final cluster centers are termed CAPs. The CAPs' sequences were obtained by labeling the original time frames according to their CAP-memberships.

Temporal dependence measurements

Following parameters were calculated based on the CAP sequence for each subject.

(1) Fraction of occurrence (FO), which is defined by:

$$FO_i = N_i/N$$

where N_i is the number of time points labeled by *i-th* CAP and N is the total number of time points of the subject. The value of FO is the activated time fraction of a CAP, and reflects its overall activity level.

(2) Transition probability, which is defined by:

$$TP_{ij} = T_{ij} / \sum_j T_{ij}$$

where T_{ij} is the number of transitions from the *i-th* CAP to the *j-th* CAP in the CAP sequence. Transition probability specifies the possibility of transition from a CAP to another CAP.

(3) Persistence: For each CAP, the average persistence (dwell time) potentially reflects the average hemodynamic response period, implying the average duration and intensity of neural activities in these regions once activated.

(4) Transition entropy, which is measured by Shannon entropy:

$$TE_i = \sum_j TP_{ij} log TP_{ij}$$

The transition entropy measures the uncertainty of transition given a current CAP depending on its transition probabilities to the other CAPs. This is a disorder metric of the temporal organization of the state space. This value would become smaller if a CAP tends to have determinate follow-up CAP(s).

(5) CAP entropy, which is also measured by Shannon entropy:

$$CE_i = \sum_i FO_i log FO_i$$

The transition entropy measures the presence uncertainty of CAPs depending on their FO values. This value would become smaller if there exist(s) dominant CAP(s), whose FO value is (are) significant larger than other CAPs.

Statistic analysis

Group wise comparisons of the CAP temporal dependence measurements were made by Student's t test. The relationships between the CAP temporal dependence measurements and CSF biomarkers were assessed by Pearson correlation coefficients and their relationships to neuropsychological scores were assessed by Spearman's correlation coefficients.

RESULTS

After removing the clusters with extreme few members, we obtained 9 CAPs with clear and specific spatial maps (Fig. 1, left column) and the co-activated regions of each CAP are listed in Table 2 (middle left column). High correspondence can be observed between the obtained CAPs and acknowledged functional networks (Table 2, middle right column), where the correlation between a CAP and a functional network were constructed when the co-activated regions contain the most core nodes of the functional network. (Bell and Shine, 2015; Bressler and Menon, 2010; Heine et al., 2012; Riedl et al., 2016; Shafiei et al., 2019; Yeo et al., 2011; Yuan et al., 2016). The relative FOs of the CAPs are also shown in Fig. 1(right column).

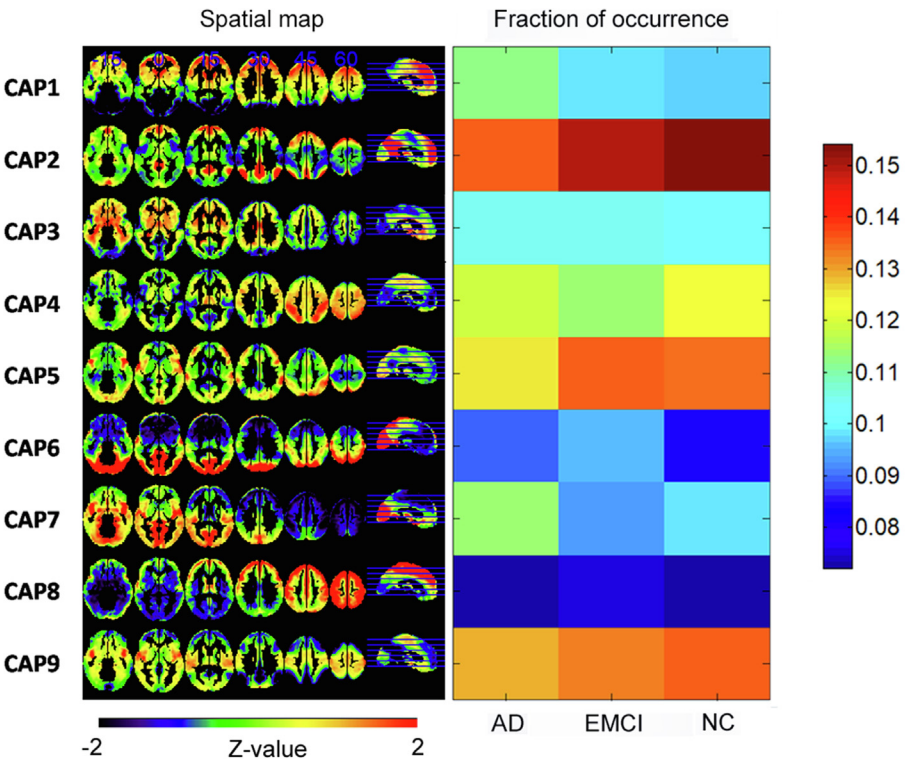

Fig. 1. Spatial maps of the obtained CAPs and their mean FOs for the three groups. Axial slice numbers in MNI space: z = −15, 0, 15, 30, 45, 60.

FO and persistence of DMN related CAP decreases from NC to AD

The DMN related CAP 2 has the highest FO among all CAPs. This reasonable as the DMN are supposed to be the primary activated network in resting state. Notably, there is a decline trend of the FO of CAP 2 from NC to EMCI and to AD. Meanwhile, the FO of CAP 9, which showing strong deactivation of DMN, also has the same decline tendency. These results implies that the "DMN

Table 2. Main co-activated brain regions of the CAPs and their relevant functional networks. These regions were identified by a brain atlas in MNI space

CAP	Activated brain regions	Relevant functional networks
1	ACC, dlPFC, mPFC, Caudate	ECN
2	PCC/Precuneus, mPFC, AG	DMN
3	Putamen, Insula, HI	SubCN
4	IPS, FEF	DAN
5	IPS, Temporal pole	—
6	Calcarine, LG, Cuneus, Precuneus, IPL	VN (dorsal)
7	Calcarine, LG, PHG, HI, Thalamus	VN (ventral)
8	PoCG, PrCG, PCL, SMA	SMN
9	Insula, SMA	SN, SMN

Key: ACC, anterior cingulated cortex; dlPFC, dorsal lateral prefrontal cortex; mPFC, medial prefrontal cortex; PCC, posterior cingulated cortex; AG, angular gyrus; HI, hippocampus; IPS, intraparietal sulcus; LG, lingual gyrus; IPL, inferior parietal lobe; PHG, parahippocampus gyrus; PoCG, postcentral gyrus; PrCG, precentral gyrus; PCL, paracentral lobe; SMA, support motor area; ECN, executive control network; DMN, default mode network; SubCN, subcortical network; DAN, dorsal attention network; VN, visual network;, SMN, sensorimotor network; SN, salience network.

collapse" discovered by conventional correlation-based FC analysis may result from the decreased frequencies of instantaneous co-activations and co-deactivations of DMN related areas. For mean persistence, significant difference was also found at CAP 2 (AD < NC, $p = 0.032$, uncorrected), where a more apparent decline trend can also be found. This indicates the decline of overall FO might arise from the shorten lifetime of each co-activation of DMN (Fig. 2a).

FO and persistence of ventral visual CAP is higher in AD than EMCI

Significant difference was found between AD and EMCI in terms of the FO of CAP 7 (AD > EMCI, $p = 0.018$, uncorrected) and the persistence of it also tends to increase from NC to EMCI and to AD, despite no statistical significance (Fig. 2a). This CAP has high spatial overlap to the ventral visual stream. In contrast, as another stream of visual information processing, the dorsal-stream related CAP 6 presents significant declined persistence for AD compared with NC group ($p = 0.046$, uncorrected) (Fig. 2a), but the no significant difference was found in terms of the FO.

OVERALL TRANSITION AND CAP ENTROPIES ARE HIGHER IN AD

Although significant difference was only found at CAP 7 (AD > EMCI, $p = 0.023$, uncorrected), the overall entropies of all the CAPs can be found higher in AD group compared to NC and EMCI (Fig. 2b). The mean CAP entropies of AD, EMCI and NC groups are 2.193 ± 0.042, 2.164 ± 0.049, and 2.172 ± 0.062, respectively, and there is significant difference between AD and EMCI groups (AD > EMCI, $p = 0.0093$, uncorrected). No significant difference was found between NC and EMCI for these two parameters.

Transition probability comparisons

The transition probability matrices of the three groups are shown in Fig. 3. For both EMCI vs. NC and AD vs. NC, significant lower CAP 9 to 4 transition probabilities was found ($p < 0.05$, uncorrected). Besides, for AD vs. NC, significant higher transition probabilities were observed for CAP 4 to 1, CAP 3 to 7 and CAP 9 to 7 ($p < 0.05$, uncorrected).

Correlations to CSF biomarkers and neuropsychological scores

The transition entropies of CAP 7 show significant negative correlation to the accumulation of Aβ while positively correlated to tau and p-tau (Fig. 4A–C). Notably, CAP 7 involves activation of parahippocampal gyrus and hippocampus. This finding implies the altered temporal organization of these CAPs may potentially attribute to the pathologically induced change of Aβ or tau accumulation in these AD-specific brain regions. Besides, the persistence of CAP 2 and 6 is found respectively correlate to p-tau and tau (Fig. 4D, E), suggesting the elevated tau accumulation plays a role in the damage of DMN especially the posterior DMN.

Total transition entropy of significantly correlated to MMSE ($r = -0.22$, $p < 0.05$, uncorrected), CDR ($r = 0.25$, $p < 0.05$, uncorrected) and FAQ ($r = 0.30$, $p < 0.01$, uncorrected), indicating this measurement may associate with a subject's overall cognitive status. Besides, the persistence of CAP 2 and 6 is found significantly correlate to CDR ($r = -0.21$ and $r = -0.23$, $p < 0.05$, uncorrected) and the persistence of CAP 7 is found significantly correlate to ADNI-MEM ($r = 0.20$, $p < 0.05$, uncorrected). The transition entropies of CAP 7 and the CAP entropy is significantly correlate to FAQ ($r = 0.22$ and $r = 0.2$, $p < 0.05$, uncorrected). No significant correlation is found between proposed measurements and GDS or ADNI-EF.

Reproducibility of the CAPs

K-means clustering has the problem of local minimum. To estimate the reproducibility of the present study, we additionally repeated the clustering for 4 times to compare with our primary trial. Specifically, for all the CAPs obtained in each repetition trail, we computed their activation area overlapping rates on the referring CAP 1–9 shown in Fig. 1. Table 3 collects the rates obtained from the repetitions. Repetition 1 resulted in very similar CAPs to our primary results, in that the clustering fell into almost the same local minimum as our primary trail. The rest 3 repetitions revealed that the CAP 2, 6, 7 were the most stable CAP, because the overlapping rates across trails are all beyond 80%. CAP 3, 4 and 9 could also be reproduced well, with the overlapping rates beyond 60%. CAP 1 and 8 could be reproduced but were not as stable as former CAPs, with the overlapping rates range from 30% to 70%. Only CAP 5 was poorly reproduced, with the overlapping rates at about 30%. Further investigation revealed that the reproducibility is partly correlated with the intra-

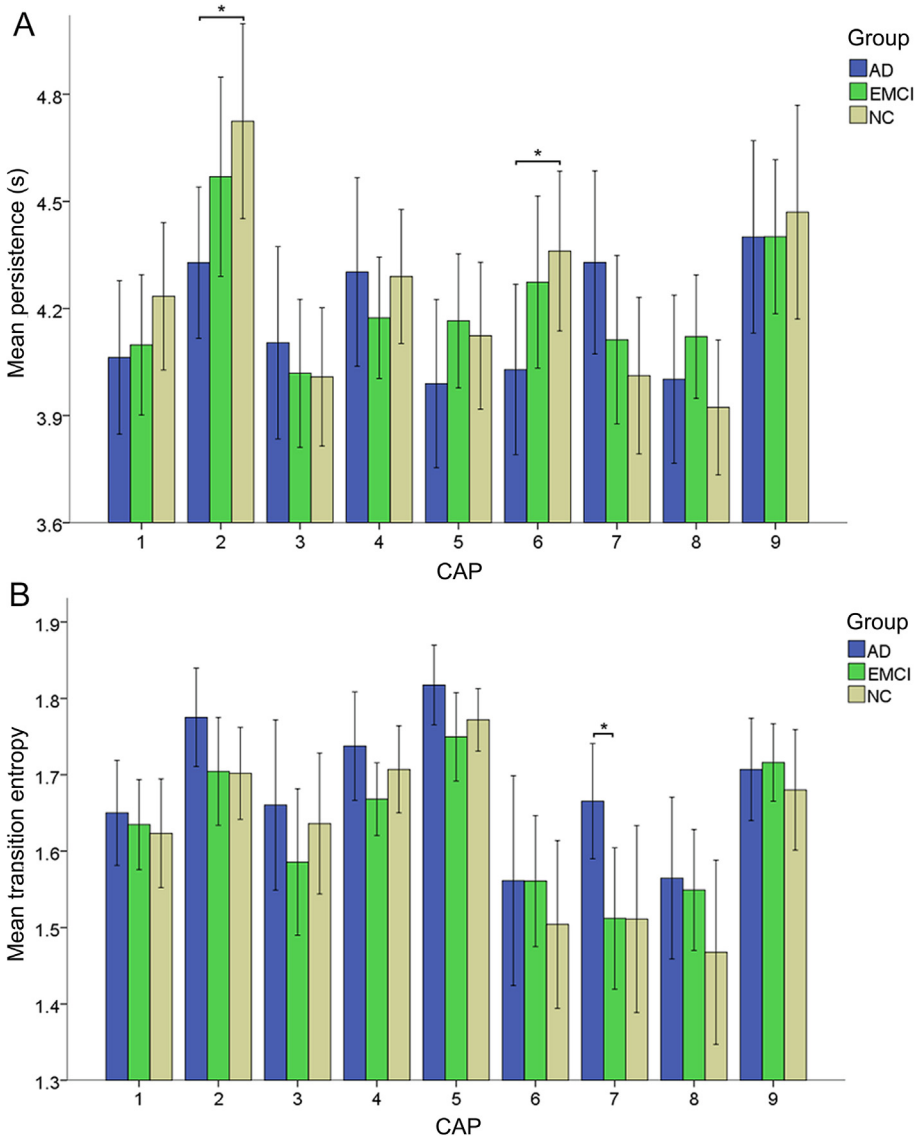

Fig. 2. (A) Mean persistence and **(B)** mean transition entropy of the CAPs for the three groups. *Statistical significant ($p < 0.05$, uncorrected).

cluster spatial similarity, in terms of which the CAP 5 has the lowest value among all the CAPs.

DISCUSSION

In this study, we validated the information provided by traditional FC analysis could condense into a set of CAPs and further temporal dependence analyses revealed AD related alterations of brain functional dynamics. In general, the primary findings include the decreased FO and mean persistence of DMN related CAPs, the increased/decreased mean persistence of ventral/dorsal visual network in disease progression, the higher transition and CAP entropies in AD group, and the multiple changes of transition probabilities. In this section, we discuss these findings based on existing studies, and try to inspire new thoughts about the abnormal brain dynamics in AD.

DMN damage in the AD progression

The decline of the FO of DMN related CAPs is in line with the previous findings, demonstrating the progressive DMN damage from the early MCI to the late dementia stage. Multiple imaging approaches have converged to imply DMN disruption in AD progression (Buckner et al., 2008). Researches of resting glucose metabolism revealed the earliest evidence that the default network is disrupted in AD. The pattern of hypo-metabolism shows great similarity to the posterior regions of the DMN (Buckner et al., 2005), and hypo-metabolism in AD progression was previously reported to be related to the patients' mental status (Herholz et al., 2002). In addition, patients with genetic risk of AD also present similar metabolism difference in DMN, suggesting that these changes may occur at the early stage of disease (Reiman et al., 1996). Structural atrophy was discovered in DMN and medial temporal subsystem (Ma et al., 2016; Thompson et al., 2003) and accelerated at the pre-clinical AD stage (Buckner et al., 2005). Task fMRI studies found the AD patients showed significantly attenuated task-induced deactivation of DMN (Celone et al., 2006; Lustig et al., 2003), and many resting state fMRI studies have reported the changes of intrinsic activity correlations among DMN regions (Celone et al., 2006; Wu et al., 2011).

Interestingly, we found the overall DMN disruption might be mainly associated with the shorten persistence of each time of DMN co-activation. Although rarely reported in the literature, we suspect this is also related to the reduction of glucose metabolism (Minoshima et al., 1997) and the build of Aβ protein (Buckner et al., 2005) in the DMN areas, because our results indicate that the persistence of DMN related CAPs decreases with the deposition of Aβ. These effects ultimately lead to the reduction of haemodynamic response and less blood flow, which may shorten duration of high blood-oxygen-level dependent signal when these areas are activated.

We also found that the DMN did not show salient co-activation with hippocampus as illustrated by CAP 2. Instead, the hippocampus was more likely to be co-activated with subcortical network and ventral visual network, i.e., the CAP 3 and CAP 7. This result appears to be not coincident with a previous independent

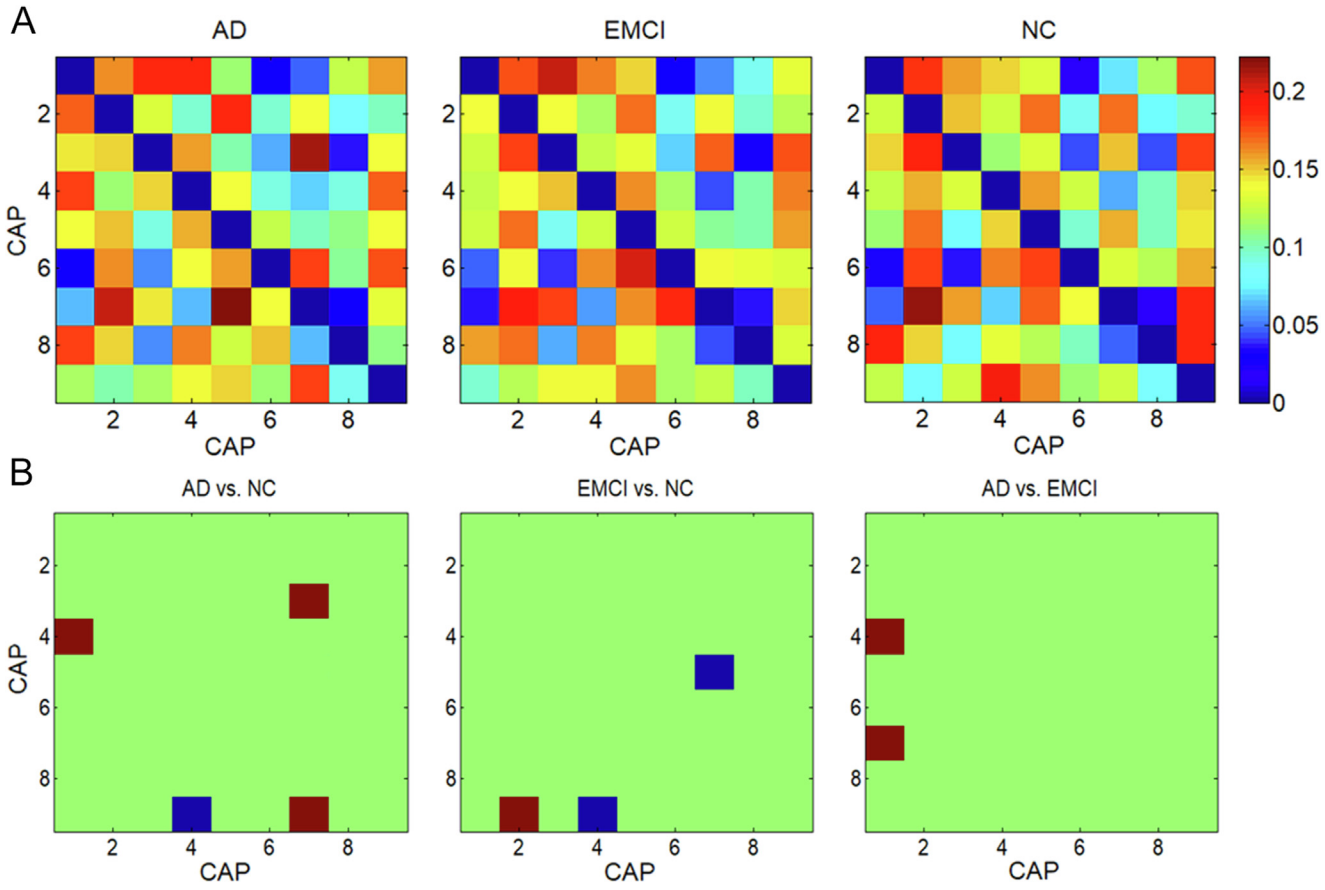

Fig. 3. (A) Transition probability (from CAPs along Y axis to CAPs along X axis) matrices of the three groups. The sum of each row is 1. **(B)** Pairwise group comparisons of their transition probability matrices, a blue/red block represents significant lower/higher ($p < 0.05$, uncorrected) transition probability.

component analysis (ICA) based study (Greicius et al., 2004) which reported the co-activation of DMN, medial temporal lobe and hippocampus in healthy elderly. However, the definition of ‘‘co-activation” in their study actually means these structures belong to the same component (with similar temporal behavior), which is different from us. If we look at the transition probability matrices presented in Fig. 3a of this study, we can find the follow-up CAP of CAP 7 has higher probability to be CAP 2 for all the three groups. Therefore, we speculate the activation of hippocampus and DMN is not simultaneously but successively with a short delay, and this may correspond to a process that the information of memory and perception from visual network and hippocampus flows into the DMN functional hub such as PCC/Precuneus.

The role of visual networks in AD

Deterioration of higher-order visuospatial abilities has been recognized in AD as an early and prominent clinical sign. Although the neurophysiologic basis remains debatable, previous visual task based studies (Franceschi et al., 2007; Paxton et al., 2007) mostly suggested this was attributed to the dysfunction of the ventral visual stream, also known as visuoperceptual stream, due to its cognitive relevance. However, in this study, at resting state, the FO and persistence of the ventral visual stream related CAP 7 was found significantly higher in AD than EMCI and also tend to be higher than NC, which indicated the enhanced activity in these regions in AD. This seems contradictory to the experience from previous studies. One explanation is that the activation of visual cortex is essentially different in rest and task; but we incline to another hypothesis that the function of the visuoperceptual stream itself is preserved in AD type dementia. Indirect supporting evidence includes the significant better performance of AD patients than dementia with Lewy bodies (DLB) patients in visual perception tasks (Mitolo et al., 2016; Wood et al., 2013a,b). Besides, a very recent fMRI research (Krajcovicova et al., 2017) reported the altered interaction between PCC/Precuneus and visuoperceptual network in MCI and AD compared with NC in a visual task. This implied the dysfunction of high-order visual processing presented in AD and MCI patients might come from an inefficient communicating mechanism between these regions.

In addition, we found the mean persistence of dorsal visual stream related CAP 6 was significantly lower in AD than NC, however, patients with AD did not show significant lower but even slightly higher mean FO than NC. This implies that the areas of dorsal visual stream may also have decreased haemodynamic responses

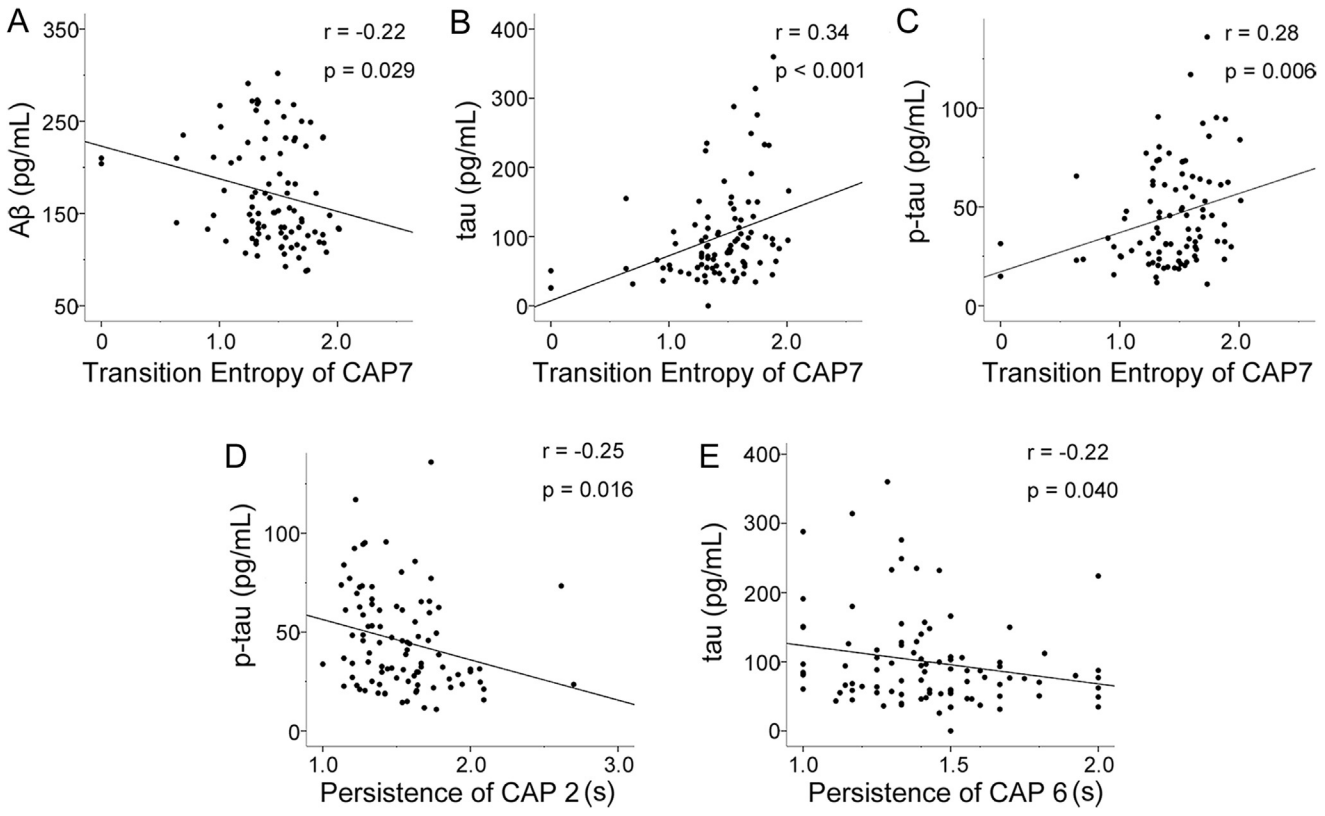

Fig. 4. (A-C) Correlations between the transition entropy of CAP 7 and CSF biomarkers. **(D-E)** Correlations between the persistence of CAP 2 and 6 and CSF biomarkers.

Table 3. Overlapping rates of the corresponding CAPs between the repetitions and the CAP 1–9 present in Fig. 1

CAP	Rep1	Rep2	Rep3	Rep4
1	0.90	0.5	0.53	0.74
2	0.93	0.83	0.84	0.89
3	0.87	0.6	0.57	0.72
4	0.87	0.53	0.7	0.77
5	0.62	0.28	0.32	0.3
6	0.97	0.8	0.82	0.87
7	0.86	0.92	0.88	0.82
8	0.62	0.5	0.56	0.38
9	0.91	0.69	0.78	0.88

Key: Rep, repetition.

when being activated in AD but they were more frequently visited. The pathophysiological mechanism of such interesting alterations in visual networks remains further study and validation.

The correlation between visual and network related CAPs and the CSF biomarkers

Elevated overall system uncertainty in AD

Interestingly, AD patients showed overall higher transition entropies for the most CAPs, especially for CAP 7 (Fig. 2b), which involves visual areas, temporal cortex and hippocampus. In the perspective of information theory, these elevated entropies may indicate the system has higher state transition uncertainties. In other words, the mode of information flow in AD brains might have changed. The significant change of the transition entropy of CAP 7 may reflect, in AD brains, the functional modules for processing the information from visual-perceptual stream and hippocampus may have essentially changed compared with NC and EMCI. Further, as indicated by the correlation of this parameter to the CSF biomarkers, we speculate that the elevated tau accumulation in CSF and the Aβ deposition in the temporal cortex and hippocampus, which have disrupted the connections or cause the death of neurons, might be the pathological basis of the altered information flow-mode in these areas.

Possible interpretations of the CAP transition probability alterations

The comparisons of AD vs. NC and EMCI vs. NC both revealed the lower CAP 9 to 4 transition probability. Noticed this is accompanied by lifted probabilities of CAP 9 to 2 for EMCI and CAP 9 to 7 for AD (Fig. 3b). In other words, the chance of triggering DAN by SN is reduced; instead there is more chance to trigger DMN and visual-perceptual networks. This change may serve as a biomarker for early disease diagnosis. Interestingly, it reminds us of a latest perspective suggesting the SN mediates the switch between DMN and central executive network (including posterior parietal cortex and dlPFC) under emotional or sensory stimuli (Uddin,

2015). We consider these altered transition probabilities for SN related CAP 9 may relate to the changed ‘‘switching” mechanism of SN, of which the dysfunction has been observed to exist in AD (He et al., 2014).

Another common change identified by AD vs. EMCI and AD vs. NC is the elevated CAP 4 to 1 transition probability. This enhanced DAN to ECN pathway may have potential disease progression relevance. Researchers have suggested that the executive dysfunction of AD is linked with connectivity change in ECN related regions. Specifically, most previous studies (Agosta et al., 2012; Anor et al., 2016; Seeley et al., 2007; Zhao et al., 2018) found increased connectivity between regions of the left executive network in patients with AD. A recent study (Cai et al., 2017) even revealed the effective connection patterns of ECN core regions and some specific connection circuit in ECN were different across MCI progressors and non-progressors.

Possible biological mechanisms of the CAPs

CAP method regards fMRI signals as a result from brief and temporally isolated events of neural activity, rather than continuous, ongoing oscillations assumed by traditional correlation analysis or ICA (Liu et al., 2018). Basically, a single fMRI image depicts in which regions the blood oxygen metabolizing level (directly correlate to the intensity of neural activity) is high. Some of the co-activated regions are intrinsically and closely connected across which the neural activity could rapidly (within an fMRI time slice) spread. Such regions could thus compose an intrinsic functional network. There are many electrophysiological evidences supporting the neural excitation and inhibition could be aroused and spread over the cortex within time of hundreds of milliseconds, via local neuronal networks and nerve fibers connecting remote regions (Luczak et al., 2007; Massimini et al., 2004; Murphy et al., 2009b). However, for each specific time slice, not all the co-activated regions are from the same network. Regions with intrinsic connectivity are more likely to show recurring co-activation over time. Therefore, we could to reconstruct these intrinsic functional networks by clustering on numerous fMRI frames. In other words, the clustering process for CAP construction is actually a ‘‘filtering” process to extract the intrinsic functional networks from the ‘‘noisy” individual fMRI images. Start from the above neurophysiological understanding of CAP, we believe that the analysis of CAP sequences could reflect many aspects of neural activity in functional networks, such as its intensity, dwell time and cross-transition mode.

Some issues about state-space models

Among the emerging state-space models, CAP method should be the simplest one which requires very few assumptions. The original CAP study (Liu and Duyn, 2013) aimed to account for the connectivity fluctuation of functional network such as DMN using a set of CAPs. However, only spatial variations across these CAPs were studied while the temporal dependence among the CAPs has not been well documented yet. In this study, the temporal dependence of CAPs was estimated by multiple parameters calculated retrospectively after the clustering process. A previous study also explores such temporal dependence using a HMM–Gaussian model (Vidaurre et al., 2017). In their study, both node (obtained by ICA) activation levels and their FC were modeled into the states, and their transition probabilities were updated iteratively to drive the inference process. Functional networks such as DMN and visual networks could also be observed by their model and can be further classified into two meta-states. Following the instruction of their toolbox, we applied their method to the data in this study. However, it turned out the sample size (total number of time points) in this study might not be sufficient to generate stable results using their model. Compared to the HMM–Gaussian model, CAP method are more convenient to apply due to much fewer model parameters. Another very recent study (Iraji et al., 2018) proposed a hierarchical state-space model to investigate brain dynamics both spatially and temporally. Their method can be regard as a combination of ICA and CAP methods, where the ICA was used to extracted intrinsic functional networks to construct a set of function domains (FDs) via a semi-automatic procedure and the k-means clustering was used to identify a set of different spatial states for each FD. By this way, they obtained subject-wise state sequences for each FD. Different from our method and the HMM–Gaussian method, they assumed multiple spatial states from different FDs could be activated simultaneously, so that each time-frame was a mixture of these states. These two state-space models both suggested hierarchical structure of the brain dynamics, while the former observed this structure from their results and the latter just directly adopted a hierarchical model. State-space approaches are convenient to combine with a hierarchical design, which is effective at the most time, to analyze the dynamics of complex system like human brain.

No matter how a state-space model is organized, it is important to control the complexity of it, especially for choosing appropriate number of states. Too many states may lead to poor signal to noise ratio and reproducibility for single state, and result in poor reliability for the following quantitatively analyses. Currently, though some automatic techniques (Damaraju et al., 2014; Vidaurre et al., 2017) are available for k choosing, we thought the supervision of researchers remains indispensable for practical applications.

In summary, CAPs with high correspondence to the functional networks defined by traditional FC analysis could be robustly observed no matter in AD, EMCI or NC group. Multiple differences were identified across the three groups in terms of the temporal dependence of the CAPs. We provide a new perspective to explain the brain functional alterations in AD and further proposed several interesting biomarkers for assisting AD treatment and early diagnosis.

ACKNOWLEDGEMENTS

Data collection and sharing for this project was funded by the Alzheimer’s Disease Neuroimaging Initiative (ADNI)

(National Institutes of Health Grant U01 AG024904) and DOD ADNI (Department of Defense award number W81XWH-12-2-0012). ADNI is funded by the National Institute on Aging, the National Institute of Biomedical Imaging and Bioengineering, and through generous contributions from the following: AbbVie, Alzheimer's Association; Alzheimer's Drug Discovery Foundation; Araclon Biotech; BioClinica, Inc.; Biogen; Bristol-Myers Squibb Company; CereSpir, Inc.; Cogstate; Eisai Inc.; Elan Pharmaceuticals, Inc.; Eli Lilly and Company; EuroImmun; F. Hoffmann-La Roche Ltd and its affiliated company Genentech, Inc.; Fujirebio; GE Healthcare; IXICO Ltd.; Janssen Alzheimer Immunotherapy Research & Development, LLC.; Johnson & Johnson Pharmaceutical Research & Development LLC.; Lumosity; Lundbeck; Merck & Co., Inc.; Meso Scale Diagnostics, LLC.; NeuroRx Research; Neurotrack Technologies; Novartis Pharmaceuticals Corporation; Pfizer Inc.; Piramal Imaging; Servier; Takeda Pharmaceutical Company; and Transition Therapeutics. The Canadian Institutes of Health Research is providing funds to support ADNI clinical sites in Canada. Private sector contributions are facilitated by the Foundation for the National Institutes of Health (www.fnih.org). The grantee organization is the Northern California Institute for Research and Education, and the study is coordinated by the Alzheimer's Therapeutic Research Institute at the University of Southern California. ADNI data are disseminated by the Laboratory for Neuro Imaging at the University of Southern California.

REFERENCES

Agosta F, Pievani M, Geroldi C, Copetti M, Frisoni GB, Filippi M (2012) Resting state fMRI in Alzheimer's disease: beyond the default mode network. Neurobiol Aging 33(8):1564–1578. https://doi.org/10.1016/j.neurobiolaging.2011.06.007.

Anor CJ, Multani N, Lake A, Moy S, Misquitta K, O'Connor S, et al. (2016) Differences in executive control network in patients with Alzheimer's disease post-aerobic exercise intervention. Alzheimer's Dementia 12(7 Supplement):P1068–P1069. https://doi.org/10.1016/j.jalz.2016.06.2234.

Banks SJ, Zhuang XW, Bayram E, Bird C, Cordes D, Caldwell JZK, et al. (2018) Default mode network lateralization and memory in healthy aging and Alzheimer's disease. J Alzheimers Dis 66 (3):1223–1234. https://doi.org/10.3233/Jad-180541.

Bell PT, Shine JM (2015) Estimating large-scale network convergence in the human functional connectome. Brain Connect 5(9):565–574. https://doi.org/10.1089/brain.2015.0348.

Belleville S, Fouquet C, Hudon C, Zomahoun HTV, Croteau J, Identification CE (2017) Neuropsychological measures that predict progression from mild cognitive impairment to Alzheimer's type dementia in older adults: a systematic review and meta-analysis. Neuropsychol Rev 27(4):328–353. https://doi.org/10.1007/s11065-017-9361-5.

Boland RJ (2015) DSM-5 (R) guidebook: the essential companion to the diagnostic and statistical manual of mental disorders, 5th edition. J Psychiatr Pract 21(2):171–173.

Bressler SL, Menon V (2010) Large-scale brain networks in cognition: emerging methods and principles. Trends Cogn Sci 14 (6):277–290. https://doi.org/10.1016/j.tics.2010.04.004.

Buckner RL, Andrews-Hanna JR, Schacter DL (2008) The brain's default network - Anatomy, function, and relevance to disease. Year Cogn Neurosci 2008(1124):1–38. https://doi.org/10.1196/annals.1440.011.

Buckner RL, Snyder AZ, Shannon BJ, LaRossa G, Sachs R, Fotenos AF, et al. (2005) Molecular, structural, and functional characterization of Alzheimer's disease: evidence for a relationship between default activity, amyloid, and memory. J Neurosci 25(34):7709–7717. https://doi.org/10.1523/Jneurosci.2177-05.2005.

Cai SP, Peng YL, Chong T, Zhang Y, von Deneen KM, Huang LY, Neuroimaging AD (2017) Differentiated effective connectivity patterns of the executive control network in progressive MCI: a potential biomarker for predicting AD. Curr Alzheimer Res 14 (9):937–950. https://doi.org/10.2174/1567205014666170309120200.

Celone KA, Calhoun VD, Dickerson BC, Atri A, Chua EF, Miller SL, et al. (2006) Alterations in memory networks in mild cognitive impairment and Alzheimer's disease: an independent component analysis. J Neurosci 26(40):10222–10231. https://doi.org/10.1523/Jneurosci.2250-06.2006.

Chang C, Glover GH (2010) Time-frequency dynamics of resting-state brain connectivity measured with fMRI. Neuroimage 50 (1):81–98. https://doi.org/10.1016/j.neuroimage.2009.12.011.

Damaraju E, Allen EA, Belger A, Ford JM, McEwen S, Mathalon DH, et al. (2014) Dynamic functional connectivity analysis reveals transient states of dysconnectivity in schizophrenia. Neuroimage-Clin 5:298–308. https://doi.org/10.1016/j.nicl.2014.07.003.

Franceschi M, Caffarra P, De Vreese L, Pelati O, Pradelli S, Savare R, et al. (2007) Visuospatial planning and problem solving in Alzheimer's disease patients: a study with the Tower of London Test. Dement Geriatr Cogn Disord 24(6):424–428. https://doi.org/10.1159/000109827.

Gibbons LE, Carle AC, Mackin RS, Harvey D, Mukherjee S, Insel P, et al. (2012) A composite score for executive functioning, validated in Alzheimer's Disease Neuroimaging Initiative (ADNI) participants with baseline mild cognitive impairment. [Research Support, N.I.H., Extramural Research Support, Non-U.S. Gov't Validation Studies]. Brain Imaging Behav 6(4):517–527. https://doi.org/10.1007/s11682-012-9176-1.

Greicius MD, Srivastava G, Reiss AL, Menon V (2004) Default-mode network activity distinguishes Alzheimer's disease from healthy aging: Evidence from functional MRI. PNAS 101(13):4637–4642. https://doi.org/10.1073/pnas.0308627101.

He XX, Qin W, Liu Y, Zhang XQ, Duan YY, Song JY, et al. (2014) Abnormal salience network in normal aging and in amnestic mild cognitive impairment and Alzheimer's disease. Hum Brain Mapp 35(7):3446–3464. https://doi.org/10.1002/hbm.22414.

Heine L, Soddu A, Gomez F, Vanhaudenhuyse A, Tshibanda L, Thonnard M, et al. (2012) Resting state networks and consciousness: alterations of multiple resting state network connectivity in physiological, pharmacological, and pathological consciousness States. Front Psychol 3:295. https://doi.org/10.3389/fpsyg.2012.00295.

Herholz K, Salmon E, Perani D, Baron JC, Holthoff V, Frolich L, et al. (2002) Discrimination between Alzheimer dementia and controls by automated analysis of multicenter FDG PET. Neuroimage 17 (1):302–316. https://doi.org/10.1006/nimg.2002.1208.

Hutchison RM, Womelsdorf T, Allen EA, Bandettini PA, Calhoun VD, Corbetta M, et al. (2013) Dynamic functional connectivity: Promise, issues, and interpretations. Neuroimage 80:360–378. https://doi.org/10.1016/j.neuroimage.2013.05.079.

Iraji A, Fu Z, Damaraju E, DeRamus TP, Lewis N, Bustillo JR, et al. (2018) Spatial dynamics within and between brain functional domains: a hierarchical approach to study time-varying brain function. Human Brain Mapp:1–18. https://doi.org/10.1002/hbm.24505.

Krajcovicova L, Barton M, Elfmarkova-Nemcova N, Mikl M, Marecek R, Rektorova I (2017) Changes in connectivity of the posterior default network node during visual processing in mild cognitive impairment: staged decline between normal aging and Alzheimer's disease. J Neural Transm 124(12):1607–1619. https://doi.org/10.1007/s00702-017-1789-5.

Liu X, Duyn JH (2013) Time-varying functional network information extracted from brief instances of spontaneous brain activity.

PNAS 110(11):4392–4397. https://doi.org/10.1073/pnas.1216856110.
Liu X, Zhang NY, Chang CT, Duyn JH (2018) Co-activation patterns in resting-state fMRI signals. Neuroimage 180:485–494. https://doi.org/10.1016/j.neuroimage.2018.01.041.
Luczak A, Bartho P, Marguet SL, Buzsaki G, Harris KD (2007) Sequential structure of neocortical spontaneous activity in vivo. PNAS 104(1):347–352. https://doi.org/10.1073/pnas.0605643104.
Lustig C, Snyder AZ, Bhakta M, O'Brien KC, McAvoy M, Raichle ME, et al. (2003) Functional deactivations: change with age and dementia of the Alzheimer type. PNAS 100(24):14504–14509. https://doi.org/10.1073/pnas.2235925100.
Ma XY, Li ZX, Jing B, Liu H, Li D, Li HY, A.S.D. Neuroimaging (2016) Identify the atrophy of Alzheimer's disease, mild cognitive impairment and normal aging using morphometric MRI analysis. Front Aging Neurosci 8. https://doi.org/10.3389/Fnagi.2016.00243 243.
Massimini M, Huber R, Ferrarelli F, Hill S, Tononi G (2004) The sleep slow oscillation as a traveling wave. J Neurosci 24 (31):6862–6870. https://doi.org/10.1523/Jneurosci.1318-04.2004.
McKhann GM, Knopman DS, Chertkow H, Hyman BT, Jack CR, Kawas CH, et al. (2011) The diagnosis of dementia due to Alzheimer's disease: Recommendations from the National Institute on Aging-Alzheimer's Association workgroups on diagnostic guidelines for Alzheimer's disease. Alzheimers Dementia 7(3):263–269. https://doi.org/10.1016/j.jalz.2011.03.005.
Minoshima S, Giordani B, Berent S, Frey KA, Foster NL, Kuhl DE (1997) Metabolic reduction in the posterior cingulate cortex in very early Alzheimer's disease. Ann Neurol 42(1):85–94. https://doi.org/10.1002/ana.410420114.
Mitolo M, Hamilton JM, Landy KM, Hansen LA, Galasko D, Pazzaglia F, Salmon DP (2016) Visual perceptual organization ability in autopsy-verified dementia with Lewy bodies and Alzheimer's disease. J Int Neuropsychol Soc 22(6):609–619. https://doi.org/10.1017/S1355617716000436.
Murphy K, Birn RM, Handwerker DA, Jones TB, Bandettini PA (2009a) The impact of global signal regression on resting state correlations: Are anti-correlated networks introduced? Neuroimage 44(3):893–905. https://doi.org/10.1016/j.neuroimage.2008.09.036.
Murphy M, Riedner BA, Huber R, Massimini M, Ferrarelli F, Tononi G (2009b) Source modeling sleep slow waves. PNAS 106 (5):1608–1613. https://doi.org/10.1073/pnas.0807933106.
Paxton JL, Peavy GM, Jenkins C, Rice VA, Heindel WC, Salmon DP (2007) Deterioration of visual-perceptual organization ability in Alzheimer's disease. Cortex 43(7):967–975. https://doi.org/10.1016/S0010-9452(08)70694-4.
Qi HH, Liu H, Hu HM, He HJ, Zhao XH (2018) Primary disruption of the memory-related subsystems of the default mode network in Alzheimer's disease: resting-state functional connectivity MRI study. Front Aging Neurosci 10. https://doi.org/10.3389/Fnagi.2018.00344 344.
Reiman EM, Caselli RJ, Yun LS, Chen KW, Bandy D, Minoshima S, et al. (1996) Preclinical evidence of Alzheimer's disease in persons homozygous for the epsilon 4 allele for apolipoprotein E. New Engl J Med 334(12):752–758. https://doi.org/10.1056/Nejm199603213341202.
Riedl V, Utz L, Castrillon G, Grimmer T, Rauschecker JP, Ploner M, et al. (2016) Metabolic connectivity mapping reveals effective connectivity in the resting human brain. PNAS 113(2):428–433. https://doi.org/10.1073/pnas.1513752113.
Saad ZS, Gotts SJ, Murphy K, Chen G, Jo HJ, Martin A, et al. (2012) Trouble at rest: how correlation patterns and group differences become distorted after global signal regression. Brain Connect 2:25–32. https://doi.org/10.1089/brain.2012.0080.
Seeley WW, Menon V, Schatzberg AF, Keller J, Glover GH, Kenna H, et al. (2007) Dissociable intrinsic connectivity networks for salience processing and executive control. J Neurosci 27 (9):2349–2356. https://doi.org/10.1523/Jneurosci.5587-06.2007.
Shafiei G, Zeighami Y, Clark CA, Coull JT, Nagano-Saito A, Leyton M, et al. (2019) Dopamine signaling modulates the stability and integration of intrinsic brain networks. Cereb Cortex 29 (1):397–409. https://doi.org/10.1093/cercor/bhy264.
Smith SM, Miller KL, Moeller S, Xu JQ, Auerbach EJ, Woolrich MW, et al. (2012) Temporally-independent functional modes of spontaneous brain activity. PNAS 109(8):3131–3136. https://doi.org/10.1073/pnas.1121329109.
Taghia J, Ryali S, Chen TW, Supekar K, Cai WD, Menon V (2017) Bayesian switching factor analysis for estimating time-varying functional connectivity in fMRI. Neuroimage 155:271–290. https://doi.org/10.1016/j.neuroimage.2017.02.083.
Tagliazucchi E, Balenzuela P, Fraiman D, Chialvo DR (2012) Criticality in large-scale brain fMRI dynamics unveiled by a novel point process analysis. Front Physiol 3. https://doi.org/10.3389/Fphys.2012.00015 15.
Thompson PM, Hayashi KM, de Zubicaray G, Janke AL, Rose SE, Semple J, et al. (2003) Dynamics of gray matter loss in Alzheimer's disease. J Neurosci 23(3):994–1005.
Uddin LQ (2015) Salience processing and insular cortical function and dysfunction. Nat Rev Neurosci 16(1):55–61. https://doi.org/10.1038/nrn3857.
Vidaurre D, Smith SM, Woolrich MW (2017) Brain network dynamics are hierarchically organized in time. PNAS 114(48):12827–12832. https://doi.org/10.1073/pnas.1705120114.
Wood JS, Firbank MJ, Mosimann UP, Watson R, Barber R, Blamire AM, O'Brien JT (2013a) Testing visual perception in dementia with Lewy bodies and Alzheimer disease. Am J Geriatr Psychiatry 21(6):501–508. https://doi.org/10.1016/j.jagp.2012.11.015.
Wood JS, Watson R, Firbank MJ, Mosimann UP, Barber R, Blamire AM, O'Brien JT (2013b) Longitudinal testing of visual perception in dementia with Lewy bodies and Alzheimer's disease. Int J Geriatr Psychiatry 28(6):567–572. https://doi.org/10.1002/gps.3860.
Wu X, Li R, Fleisher AS, Reiman EM, Guan XT, Zhang YM, et al. (2011) Altered default mode network connectivity in Alzheimer's disease-A resting functional MRI and Bayesian Network Study. Hum Brain Mapp 32(11):1868–1881. https://doi.org/10.1002/hbm.21153.
Yan C, Zang Y (2010) DPARSF: a MATLAB toolbox for "pipeline" data analysis of resting-state fMRI. Front Syst Neurosci 4.
Yeo BT, Krienen FM, Sepulcre J, Sabuncu MR, Lashkari D, Hollinshead M, et al. (2011) The organization of the human cerebral cortex estimated by intrinsic functional connectivity. J Neurophysiol 106(3):1125–1165. https://doi.org/10.1152/jn.00338.2011.
Yuan R, Di X, Taylor PA, Gohel S, Tsai YH, Biswal BB (2016) Functional topography of the thalamocortical system in human. Brain Struct Funct 221(4):1971–1984. https://doi.org/10.1007/s00429-015-1018-7.
Zhao QH, Lu H, Metmer H, Li WXY, Lu JF (2018) Evaluating functional connectivity of executive control network and frontoparietal network in Alzheimer's disease. Brain Res 1678:262–272. https://doi.org/10.1016/j.brainres.2017.10.025.

(Received 13 March 2019, Accepted 15 November 2019)
(Available online 27 November 2019)